



# Material's selection rules for high performance triboelectric nanogenerators

Yang Yu <sup>1,2,#</sup>, Hengyu Li <sup>1,3,#</sup>, Da Zhao <sup>1,#</sup>, Qi Gao <sup>1,2</sup>, Xiang Li <sup>1,2</sup>, Jianlong Wang <sup>1,2</sup>, Lin Zhong Wang <sup>1,4,\*</sup>, Tinghai Cheng <sup>1,2,\*</sup>

<sup>1</sup> Beijing Institute of Nanoenergy and Nanosystems, Chinese Academy of Sciences, Beijing 101400, China

<sup>2</sup> School of Nanoscience and Technology, University of Chinese Academy of Sciences, Beijing 100049, China

<sup>3</sup> State Key Laboratory of Robotics and System, Harbin Institute of Technology, Harbin 150001, Heilongjiang Province, China

<sup>4</sup> Georgia Institute of Technology, Atlanta, GA 30332-0245, United States

Selecting suitable triboelectric materials for triboelectric nanogenerators (TENGs) with excellent integrated performance at ambient environment remains a challenge. Here, we propose a set of universal material's selection rules for TENGs with comprehensive material's properties, including surface charge density in low and high relative humidity, moisture resistance rate, and friction coefficient. The influence mechanisms of environmental factors on the output performance of TENG are first revealed. Based on the selection rules, comprehensive selection series are ranked for all types of TENGs with fifteen triboelectric material pairs (cumulative sixty sets of samples). Additionally, two TENG integrated devices are also presented to confirm the generality and feasibility of the selection rules. The moisture resistance rate reaches up to 124% after working in ambient conditions with 95% relative humidity for 36, 000 s. This work provides a significant guideline for triboelectric material's selection and promotes the practical applications of TENG.

**Keywords:** Material's selection rules; High performance; Triboelectric nanogenerator; Ambient environment

## Introduction

With the rapid depletion of global fossil energy sources and the serious pollution of the environment caused by fossil energy, developing clean and renewable energy has become a huge challenge for human beings [1,2]. Triboelectric nanogenerators (TENGs) provide a superior strategy to harvest distributed mechanical energy from natural environments, with the advantages of high conversion efficiency, a wide choice of materials, low cost, and easy fabrication, which has attracted extensive attention from research scholars [3–6]. However, their output performance depends on temperature [7–9] and humidity, espe-

cially humidity [10–12]. Improving the moisture resistance of triboelectric materials is essential to better realize the commercial applications for TENG [13]. In this regard, many strategies have been developed to increase the output capability of TENG in high humid environments. For example, TENG can maintain normal operation in high humid environments for a short time by adopting encapsulation technology to prevent water molecules into the devices [14–16]. A further strategy is to increase the hydrophobicity of triboelectric materials to prevent water molecules from adhering to their surfaces, such as nano-in-micro structures [17], layer-by-layer assembly-induced [18], particle lithography [19], and surface-charge engineering [20]. Recently, the self-polarization effect and surface lubrication techniques have also been employed to overcome humidity influences on TENG [21,22]. Although the moisture resistance of TENG devices has been greatly improved, the complicated oper-

\* Corresponding authors.

E-mail addresses: Zhong Wang, L. (zhong.wang@mse.gatech.edu), Cheng, T. (chengtinghai@binn.cas.cn).

# Yang Yu, Hengyu Li and Da Zhao contributed equally to this work.

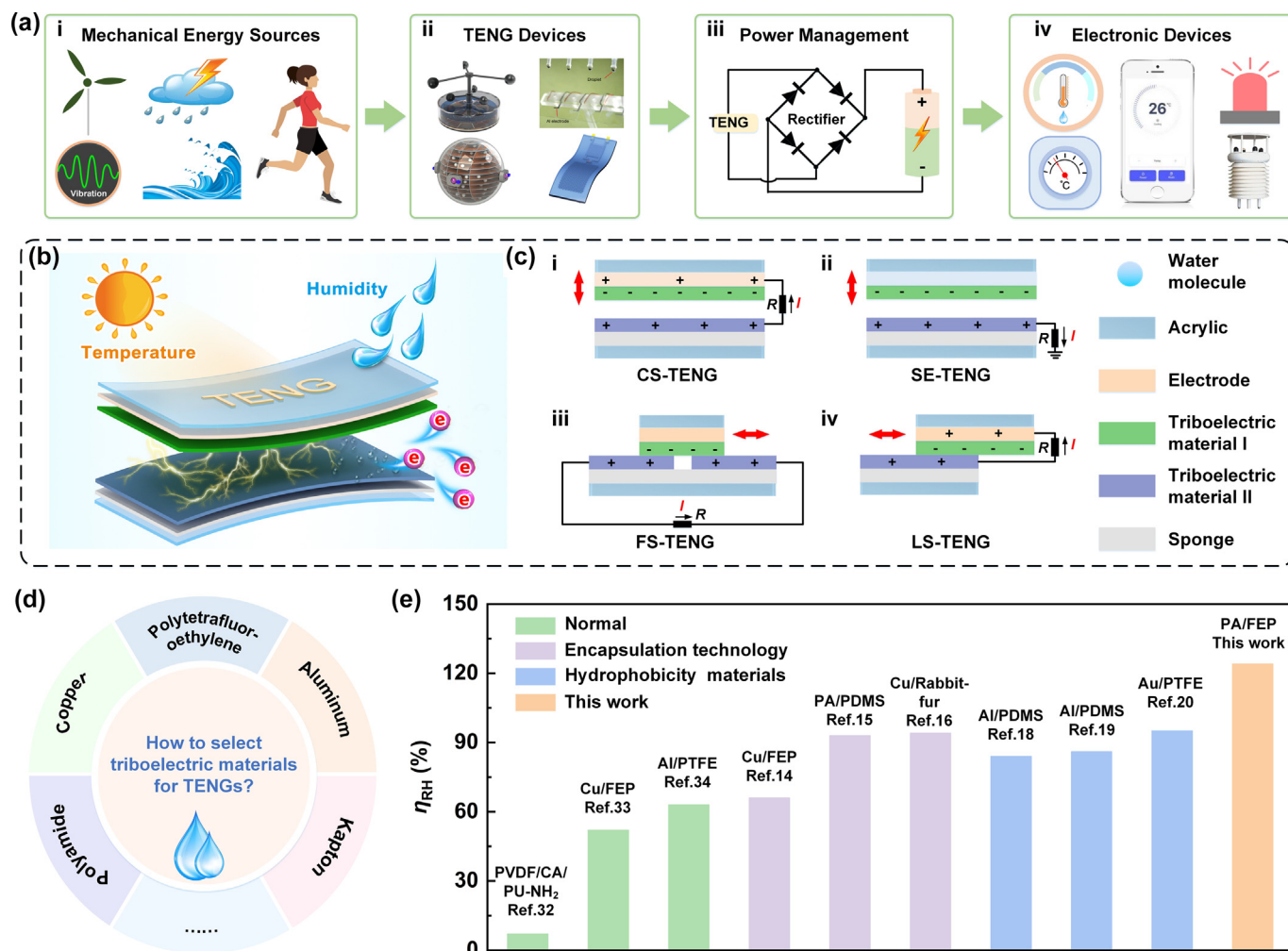


FIGURE 1

**Structures and working mechanisms of TENG.** **a** Self-powered sensing systems powered by TENG devices. **b** Triboelectric materials absorb water molecules from the surroundings and form water droplets on the surfaces. **c** Four basic working modes of TENG. **d** Materials of TENG with wide sources. **e** Comparison of the  $\eta_{RH}$  in this study with other related reports [14–16,18–20,32–34].

ation procedures and high cost have greatly limited the industrial production and practical applications of TENGs.

Triboelectric materials are the foundation of TENG devices [23], and it is particularly critical to select suitable triboelectric materials to design high performance TENG. Triboelectric series are the main available tool for selecting triboelectric materials. Most triboelectric series are determined based on the polarity of materials, which describe the tendency of materials to generate triboelectric charges [24]. Due to the complexity of experimental parameters, such as temperature, humidity, and material mechanical properties, the material's ranking in the triboelectric series as measured by different researchers shows various results. To overcome these problems, a triboelectric series determined by charge density using liquid material in nitrogen was quantified, which provides a reference to choose triboelectric materials for TENG [25,26]. This study is only applicable to constant temperature ( $20 \pm 1$  °C) and relative humidity (0.43% RH) conditions, and the research object is only for contact-separation mode TENG. In order to apply to other model of TENG, a set of selec-

tion rules of triboelectric materials for direct-current triboelectric nanogenerator (DC-TENG) have been studied [27], which offers a new idea for selecting triboelectric materials in laboratory environments. In practical applications, most TENG devices work at ambient environment with real-time changes in humidity and temperature. There is still a lack of guidance on the selection of triboelectric materials for different types of TENGs with high performance at ambient environment.

In this work, a set of selection rules are proposed to determine whether a triboelectric material pair is appropriate for TENG and to determine a selection priority by comprehensive selection series using the normalization method. The influence mechanisms of environmental factors on the output capability of TENGs are investigated. Taking the parameters (surface charge density in low and high relative humidity, moisture resistance rate, and friction coefficient), polyamide (PA) and fluorinated ethylene propylene (FEP) show superior output performance in variable humid environments. Two integrated devices are designed to prove the practicability of the selection rules. The proposed rules

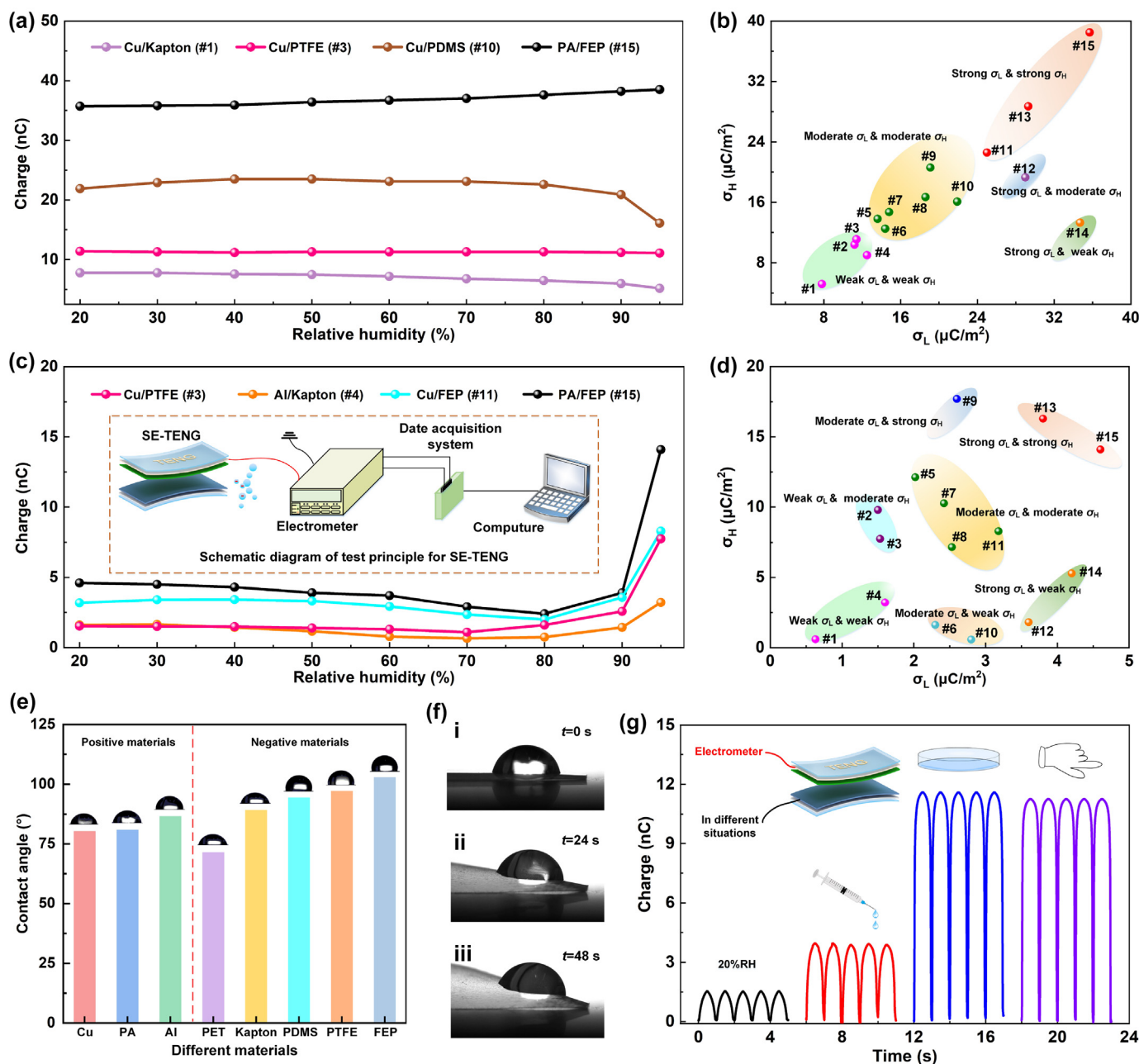


FIGURE 2

**Influence of environmental humidity on CS/SE-TENG.** **a** Transferred charge of CS-TENG in different relative humid environments. **b** The surface charge densities of CS-TENG in 20% RH and 95% RH. **c** Transferred charge of SE-TENG in different relative humid environments. **d** The surface charge densities of SE-TENG in 20% RH and 95% RH. **e** The contact angles of Cu, PA, Al, PET, Kapton, PDMS, PTFE, and FEP films. **f** Photograph of “self-deformation” of the PA film after adding water medium. **g** Transferred charge of SE-TENG when triboelectric material II contacts with variable situations.

are a comprehensive consideration for natural environments, which will provide an important guideline to design high performance TENG in practical applications and reduce the trial and error cost in selecting triboelectric materials for TENG research.

## Results

**Structures and working mechanisms of TENG.** As one of the prime candidates for powering the self-powered sensing system (Fig. 1a) [28–31], it is vital that the TENG maintains a high and stable output performance from mechanical energy

sources to electricity. However, the variation of environment in mechanical energy sources becomes a significant challenge for TENG in practical applications. As shown in Fig. 1b, the operation of TENG under the natural environment is influenced by temperature and humidity. Under high humidity environments, water molecule aggregation at the interfaces of triboelectric materials significantly affects contact electrification. TENG can be divided into four categories based on their working modes (Fig. 1c): i Contact-separation mode TENG (CS-TENG); ii Single-electrode mode TENG (SE-TENG); iii Free-standing mode

TENG (FS-TENG); iv Lateral-sliding mode TENG (LS-TENG). The detailed working mechanisms and explanations are illustrated in [Supplementary Fig. 1](#) and Note 1. Triboelectric materials for TENG have a wide range of options, including polyamide, copper, polytetrafluoroethylene, aluminum, Kapton, etc. ([Fig. 1d](#)), it is imperative to establish selection rules for selecting suitable triboelectric materials for TENG devices.

To characterize the adaptability of TENG at ambient environment, the moisture resistance rate  $\eta_{RH}$  (the ratio of the output performance in high and low relative humidity) in this study is compared with other related reports. As shown in [Fig. 1e](#), the  $\eta_{RH}$  of normal TENG devices can be varied by using different triboelectric materials. Furthermore, the  $\eta_{RH}$  using encapsulation technology and hydrophobicity materials is effectively improved, reaching a maximum of 95%. In contrast, the  $\eta_{RH}$  of the TENG device in this work achieves 124%, which is the highest in reported studies. The detailed comparison is shown in [Supplementary Table 1](#).

**The standardization of test conditions.** To determine the appropriate selection rules of triboelectric materials for TENG at ambient environment, the diverse measurement systems ([Supplementary Fig. 2](#) and Note 2) are established for different types of TENGs under well-controlled conditions, with a fixed temperature (25 °C), a contact force (2 N), and a driving frequency (1 Hz). The details of motor operating parameters are presented in [Supplementary Table 2](#). Commonly used positive materials of copper (Cu), polyamide (PA), aluminum (Al), and negative materials of polydimethylsiloxane (PDMS), polyethylene terephthalate (PET), polytetrafluoroethylene (PTFE), Kapton, fluorinated ethylene propylene (FEP) are studied. A total of 15 types of material pairs are combined, namely Cu/Kapton (#1), Cu/PET (#2), Cu/PTFE (#3), Al/Kapton (#4), Al/PET (#5), PA/Kapton (#6), Al/PTFE (#7), PA/PET (#8), PA/PTFE (#9), Cu/PDMS (#10), Cu/FEP (#11), Al/PDMS (#12), Al/FEP (#13), PA/PDMS (#14), PA/FEP (#15). Detailed information on the test materials can be found in [Supplementary Table 3](#). To determine accurate selection rules, It should be known how ambient temperature and humidity affect the output performance of TENG. As shown in [Supplementary Fig. 3](#), when the temperature changes from  $-10$  °C to  $40$  °C, the output capacity of the TENG is almost unaffected. So, the influence of humidity on TENG should be systematically researched.

**Influence of environmental humidity on CS/SE-TENG.** The transferred charge of CS-TENG with 15 kinds of triboelectric material pairs in 20% RH is shown in [Supplementary Fig. 4](#). The transferred charge of CS-TENG under different humid environments is investigated in [Supplementary Fig. 5](#). As the relative humidity increases, the transferred charge shows four types of variation laws: a. continuous decrease (e.g., #1, #4, #6 and #11); b. remained stable (e.g., #3 and #7); c. first increase and then decrease (e.g., #2, #5, #8, #10, #12, #13, and #14); d. continuous increase (e.g., #9 and #15). Typical triboelectric material pairs #1, #3, #10, and #15 are selected as shown in [Fig. 2a](#). The output performance of CS-TENG can be maintained or improved in variable humid environments by selecting appropriate triboelectric materials. The optimum working humidity for CS-TENG with different material pairs is illustrated in [Supplementary Fig. 6a](#).

The surface charge densities  $\sigma_L$  (low humidity of 20% RH) and  $\sigma_H$  (high humidity of 95% RH) of CS-TENG with different triboelectric material pairs are shown in [Fig. 2b](#). It can be seen that #12 and #14 have relatively high  $\sigma_L$  but moderate and low  $\sigma_H$ . Thus, they are not suitable as triboelectric materials in practical applications. Except for them, the relationship between  $\sigma_L$  and  $\sigma_H$  can be divided into three types: a. weak  $\sigma_L$  with weak  $\sigma_H$  (e.g., #1, #2, #3, and #4); b. moderate  $\sigma_L$  with moderate  $\sigma_H$  (e.g., #5, #6, #7, #8, #9, and #10); c. high  $\sigma_L$  with high  $\sigma_H$  (e.g., #11, #13, and #15). In general, triboelectric materials with a larger  $\sigma_L$  may tend to have a larger  $\sigma_H$ . Therefore, the  $\sigma_L$  is an important basis for directly screening whether a material is suitable for a triboelectric material. The  $\eta_{RH}$  of different triboelectric materials for CS-TENG is shown in [Supplementary Fig. 7a](#), which is an important parameter in the triboelectric material's selection rules for TENG. In addition, as shown in [Supplementary Fig. 8a](#), by selecting different material pairs, the surface charge densities of TENG devices show different changing trends under variable humid environments.

The influence of environmental humidity on SE-TENG with a variety of material pairs is investigated ([Supplementary Fig. 9](#)), and a schematic diagram of the test principle is shown in the inset of [Fig. 2c](#). When the environmental humidity is less than 80% RH or 90% RH, the transferred charge of SE-TENG follows a similar change trend as that of the CS-TENG; and when the environmental humidity continues to increase, the transferred charge increases rapidly with increasing relative humidity ([Fig. 2c](#)). The optimum working relative humidity and  $\eta_{RH}$  of SE-TENG are shown in [Supplementary Fig. 6b](#) and 7b, respectively. Furthermore, the relationship between  $\sigma_L$  and  $\sigma_H$  of SE-TENG is also studied in [Fig. 2d](#). This shows that the premise of achieving a relatively high  $\sigma_H$  is generally held to be a relatively high  $\sigma_L$ , which determines whether a material is suitable as a triboelectric material. The trend of charge density with different materials under a variable humid environment is illustrated in [Supplementary Fig. 8b](#), which guides researchers to choose required triboelectric materials in practical applications.

To gain a deeper understanding of the influence of environmental humidity on the output performance of CS/SE-TENG, the contact angles ( $\theta$ ) of different triboelectric materials are tested to characterize hydrophobic properties ([Fig. 2e](#) and [Supplementary Fig. 10](#)). Generally, the triboelectric material film with a higher  $\theta$  indicates a stronger hydrophobicity and prevents the adsorption of water molecules, thus enhancing moisture resistance of TENG. The  $\theta$  are  $80.2^\circ$  for Cu film,  $80.8^\circ$  for PA film,  $86.6^\circ$  for Al film,  $71.4^\circ$  for PET film,  $89.2^\circ$  for Kapton film,  $94.3^\circ$  for PDMS film,  $97.2^\circ$  for PTFE film, and  $102.9^\circ$  for FEP film. Surprisingly, the PA film with a medium  $\theta$  shows the excellent output. This is because the PA film contains amide groups (-CONH-), which is easily hydrogen bonded to water molecules. This leads to the "self-deformation" of the PA film ([Fig. 2f](#) and [Supplementary Movie 1](#)). Under normal conditions, the actual contact area of the triboelectric materials is only a fraction of the material surface area due to the unsmooth surface of the triboelectric materials. When using the PA film in a high humid environment, the "self-deformation" will make triboelectric materials contact more fully, and the schematic diagram is shown in [Supplementary Fig. 11](#).



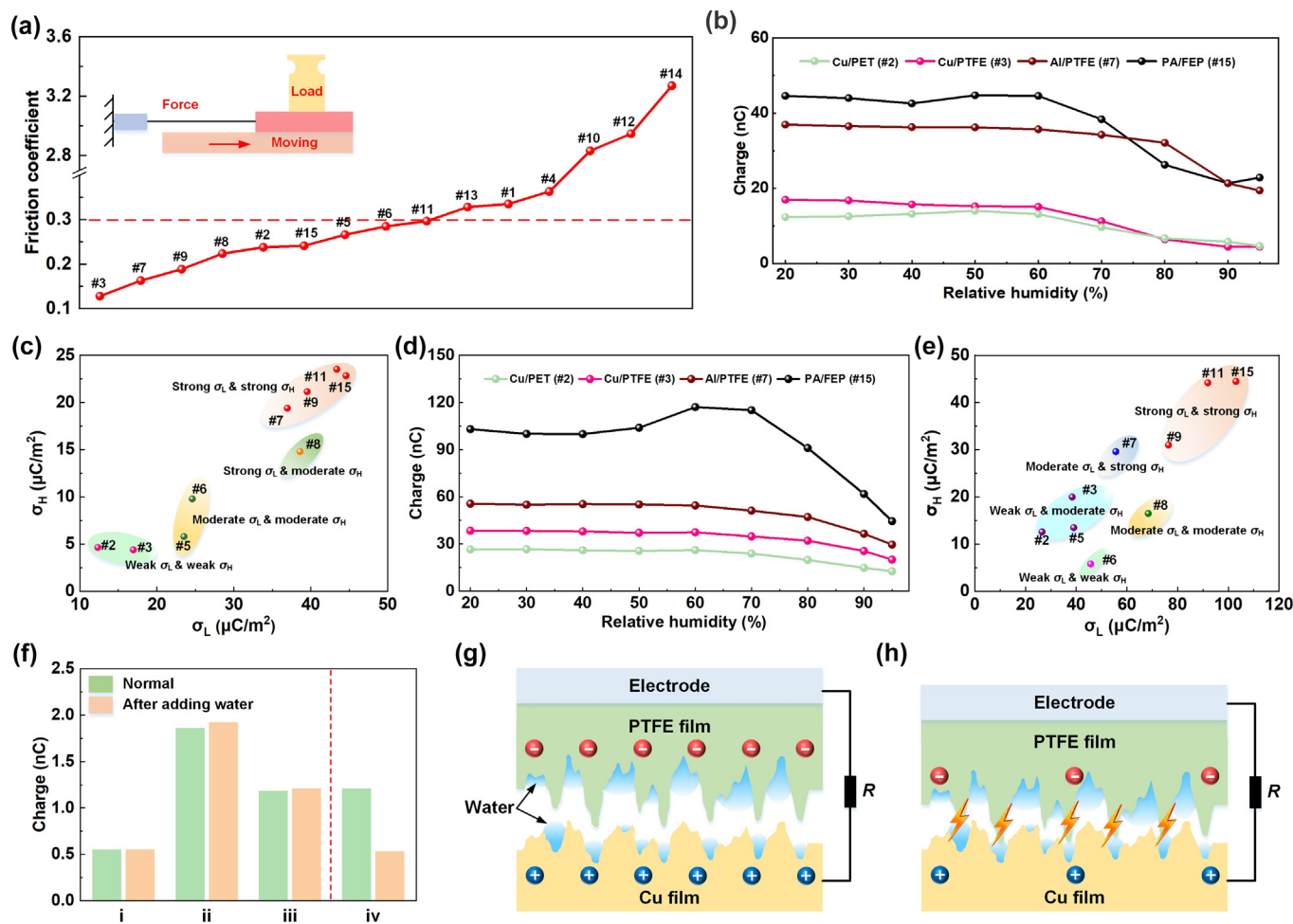


FIGURE 3

**Influence of environmental humidity on FS/LS-TENG.** **a** The friction coefficient of test materials. **b** Transferred charge of FS-TENG in different relative humid environments. **c** The surface charge densities of FS-TENG in 20% RH and 95% RH. **d** Transferred charge of LS-TENG in a variable relative humid environment. **e** The surface charge densities of LS-TENG in 20% RH and 95% RH. **f** Comparison of transferred charge of TENG in normal and after adding water with different cases. (i: CS-TENG with a large gap and water droplets are still; ii: CS-TENG with a small gap and water droplets are moving; iii: FS-TENG with a gap and water droplets are still; iv: FS-TENG with a gap and water droplets are moving.) **g** Mechanisms for the distribution of water droplets on the surface of triboelectric materials in a humid environment for CS-TENG or FS-TENG (triboelectric materials with a large gap). **h** Mechanisms for the distribution of water droplets on the surface of triboelectric materials in a humid environment for FS-TENG (triboelectric materials with a small gap or contact).

Noteworthy, SE-TENG performs better in high humid environments due to its unique working and test principle (Fig. 1c and the insert of Fig. 2c). During the testing process, only the electrode is connected to the electrometer by a wire. When the air is dry, it has a low conductivity, but as the relative humidity increases, its conductivity increases, thus increasing the number of electrons changing between material II and the air. Whenever the relative humidity is high enough, the air is equivalent to a conductor, and the SE-TENG has the maximum surface charge density. To demonstrate the above conclusion, various conductive situations are constructed (a little water, a lot of water, and a hand). A comparison is performed between the transferred charge in conductive conditions and a 20% RH environment, as shown in Fig. 2g. In the experimental results, the transferred charge of SE-TENG increases significantly in conductive situations. Transferred charge in a small amount of water is smaller because it lacks sufficient electronics.

**Influence of environmental humidity on FS/LS-TENG.** The motions of FS/LS-TENG are accompanied by a process of friction, hence selecting triboelectric materials with low friction coefficients ( $\mu$ ) is crucial for obtaining high efficiency. The  $\mu$  of different materials and the test diagram are shown in Fig. 3a. A large  $\mu$  will increase the wear of triboelectric materials during the sliding movement, so the material pairs with  $\mu$  higher than 0.3 are excluded.

The influence of relative humidity on the output performance of FS/LS-TENG is shown in Supplementary Figs. 12 and 13. To demonstrate the variation law of the transferred charge amount of FS/LS-TENG more clearly, four pairs of triboelectric materials (Cu/PET (#2), Cu/PTFE (#3), Al/PTFE (#7), PA/FEP (#15)) are selected as shown in Fig. 3b and 3d. As the relative humidity increases, the transferred charge of FS/LS-TENG initially exhibits a similar trend to that of CS/SE-TENG at first and then decreases. The surface charge densities  $\sigma_L$  and  $\sigma_H$  of FS/LS-TENG are illus-

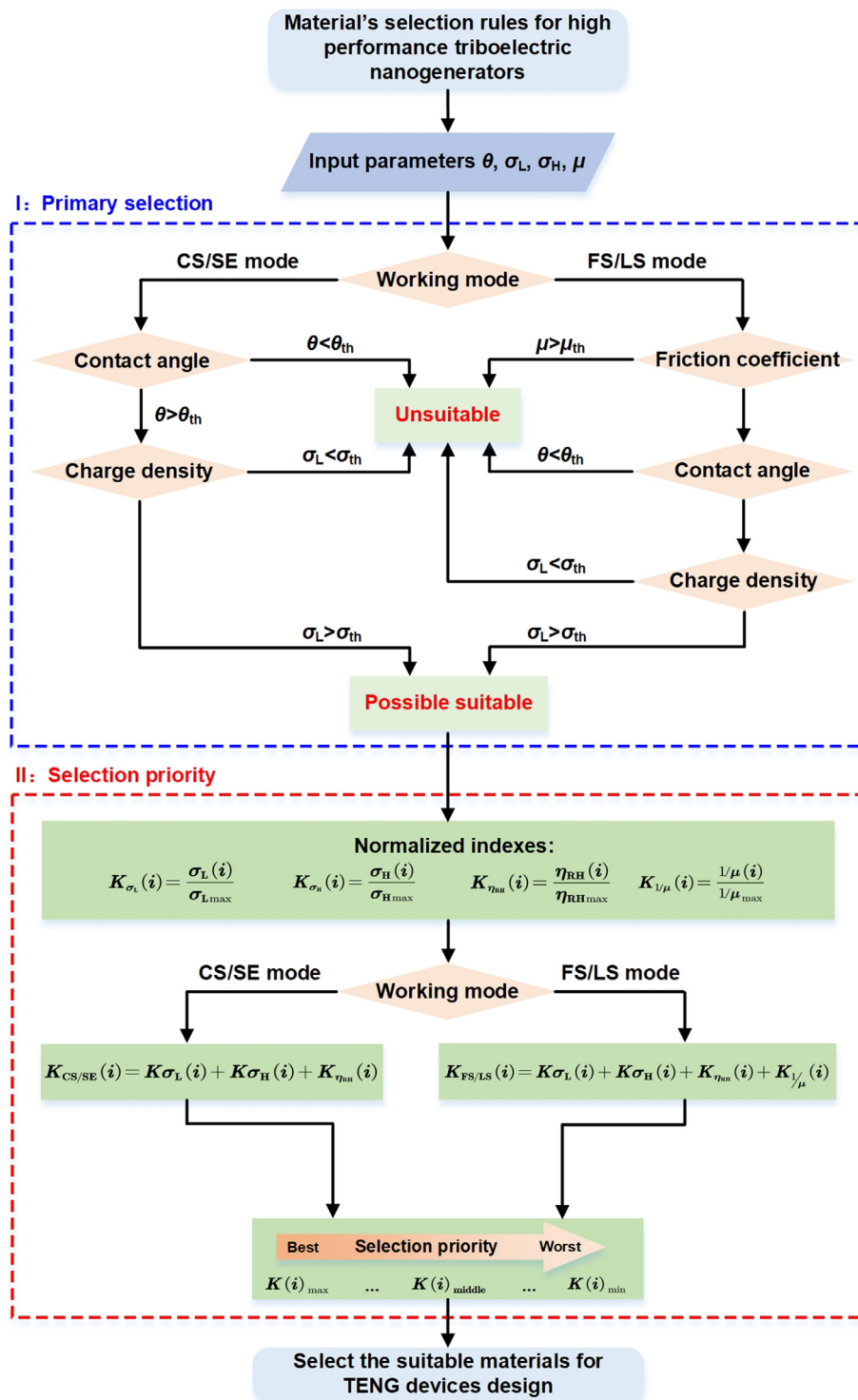


FIGURE 4

Material's selection rules for high performance triboelectric nanogenerators.

trated in Fig. 3c and 3e, respectively. The results show that although triboelectric materials usually have a better  $\sigma_H$  when they have a higher  $\sigma_L$ , this is not an absolute statement. Thus, the parameters  $\sigma_L$  and  $\sigma_H$  should be considered to accurately select appropriate material pairs. The optimum working relative

humidity and the moisture resistance rate of FS/LS-TENG are summarized in Supplementary Fig. 6c-d and 7c-d, respectively. The results show that FS/LS-TENG is more suitable for working in low humid environments. In addition, the moisture resistance of CS-TENG is compared with that of FS-TENG (Supplementary

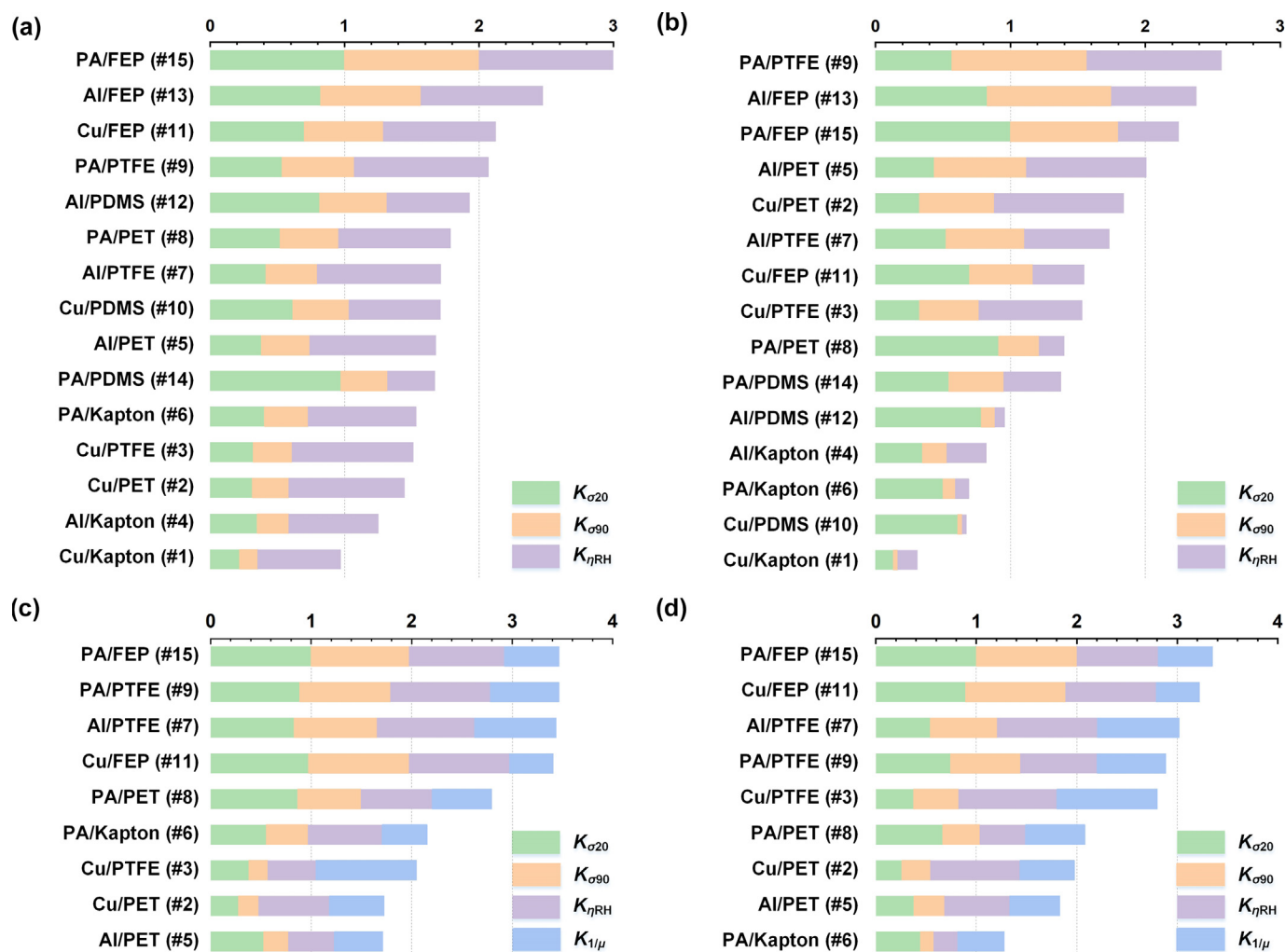


FIGURE 5

Comprehensive selection series of triboelectric materials for TENGs. **a** CS-TENG. **b** SE-TENG. **c** FS-TENG. **d** LS-TENG.

Figs. 14–15 and Supplementary Movies 2–3). When water medium is added directly to CS-TENG, the transferred charge amount remains almost stable (from 10.2 nC to 10.1 nC). In contrast, the transferred charge of FS-TENG decays sharply (from 14.6 nC to 1.4 nC).

Two potential reasons may explain the poor moisture resistance of FS/LS-TENG compared to CS/SE-TENG. On the one hand, the motion of FS/LS-TENG is a sliding movement that increases the wear of materials. On the other hand, FS/LS-TENG influences the motion of water droplets. To determine the potential reasons, the transferred charge of CS-TENG with different surface roughness is first measured by rubbing the triboelectric materials of CS-TENG with sandpaper, as shown in Supplementary Fig. 16, and the results indicate that the surface roughness (wear) of triboelectric materials has no significant effect on the performance of TENG at ambient environment. Then, different motion states of water droplets on the triboelectric material surfaces of different types of TENGs are investigated (Supplementary Fig. 17), and the corresponding transferred

charge is compared with the normal situation in Fig. 3f. Except for case iv, the transferred charge with triboelectric materials Cu/PTFE is independent of the environment humidity, even when water medium is applied directly to the surface of triboelectric materials. The result shows that the motion of water droplets is the main factor impacting the moisture resistance of TENG. This is because when TENG work in humid environments, water molecules will accumulate on the surface of triboelectric material, as shown in Supplementary Fig. 18. For CS-TENG or FS-TENG (triboelectric materials with a large gap), due to the large gaps between test triboelectric materials, there will not be a continuous water film between them, as shown in Fig. 3g. For FS-TENG (triboelectric materials with a small gap or contact), because of the surface tension of water, continuous water bridges can be formed between the triboelectric materials during the work process (Fig. 3h). In this case, the majority of electrons will be exchanged through the water bridge during operation, while only a small part of electrons will flow through the external circuit, resulting in a dramatic drop in the output

performance of the FS-TENG. Thus, the development of improving the moisture resistance of TENG should focus on FS/LS-TENG in the future.

**Material's selection rules for TENGs at ambient environment.** The material's selection rules for TENGs based on the parameters  $\theta$ ,  $\sigma_L$ ,  $\sigma_H$ , and  $\mu$  are shown in Fig. 4. This model can determine whether a material pair is appropriate as triboelectric materials for TENGs at ambient environment. In addition, it can determine the selection priority of triboelectric materials. The selection rules consist of two steps. Step I: Due to the different motion mechanisms of TENG, the working mode of TENG needs to be judged first. For CS/SE-TENG, the hydrophobic materials can prevent water molecules from adsorbing on their surfaces in high humid environments. Thus, triboelectric materials with small  $\theta$  should be excluded. Then, based on the influence mechanisms of environmental humidity for CS/SE-TENG, triboelectric materials with high  $\sigma_L$  are possibly suitable for CS/SE-TENG. For FS/LS-TENG, triboelectric materials with a suitable  $\mu$  should be considered first to reduce the wear and heat of the contact surface. Therefore, triboelectric materials with large  $\mu$  should be ignored. The process of selecting triboelectric materials with appropriate  $\theta$  and  $\sigma_L$  for FS/LS-TENG is the same as that for CS/SE-TENG. Step II: Determine the selection priority of the possible suitable triboelectric materials using the normalization method. Four parameters  $\sigma_L$ ,  $\sigma_H$ ,  $\eta_{RH}$ , and  $1/\mu$  (the reciprocal of friction coefficient) are considered. To comprehensively evaluate the triboelectric material, the four parameters of different triboelectric materials are normalized as follows:

$$K_{\sigma_L}(i) = \frac{\sigma_L(i)}{\sigma_{L\max}} \quad (1)$$

$$K_{\sigma_H}(i) = \frac{\sigma_H(i)}{\sigma_{H\max}} \quad (2)$$

$$K_{\eta_{RH}}(i) = \frac{\eta_{RH}(i)}{\eta_{RH\max}} \quad (3)$$

$$K_{1/\mu}(i) = \frac{1/\mu(i)}{1/\mu_{\max}} \quad (4)$$

where  $\sigma_{L\max}$ ,  $\sigma_{H\max}$ ,  $\eta_{RH\max}$ , and  $1/\mu_{\max}$  are the maximum of  $\sigma_L$ ,  $\sigma_H$ ,  $\eta_{RH}$ , and  $1/\mu$  of possible suitable triboelectric materials. To ensure the priority of triboelectric material's selection, the combined selection coefficients for CS/SE-TENG and FS/LS-TENG are proposed.

$$K_{CS/SE}(i) = K_{\sigma_L}(i) + K_{\sigma_H}(i) + K_{\eta_{RH}}(i)$$

$$K_{FS/LS}(i) = K_{\sigma_L}(i) + K_{\sigma_H}(i) + K_{\eta_{RH}}(i) + K_{1/\mu}(i)$$

As the above analyses, the higher the  $K_{CS/SE}(i)$  and  $K_{FS/LS}(i)$  of triboelectric materials, the higher the priority level of selection. It should be noted that the thresholds ( $\mu_{th}$ ,  $\theta_{th}$ , and  $\sigma_{th}$ ) will be redefined as additional materials are studied. Furthermore, the selection model is not limited to selecting triboelectric materials for TENGs at ambient environment, but can also be used under other alternate environments.

TENG has applications for energy harvesting and self-powered sensing. For energy harvesting type TENG, triboelectric materials

should have stable and high performance in both low and high humid environments. For sensing type TENG, triboelectric materials with stable current/voltage output are essential for the stability and accuracy of the sensors. Thus, the comprehensive selection series of triboelectric materials based on the proposed selection rules for CS/SE/FS/LS-TENG are shown in Fig. 5 (Detailed origin and normalized indexes are shown in Supplementary Tables 4–7.). It can be seen that TENG with the PA film and strong hydrophobic materials (e.g., FEP and PTFE) shows better comprehensive output performance. This selection series provides an important reference for selecting suitable triboelectric materials for TENGs at ambient environment. With further development, triboelectric materials used for TENGs will be further enriched. The selection rules are not limited to the above material pairs but are also used for any other triboelectric materials.

**Applications of selected triboelectric materials for TENG integrated devices.** CS-TENG and FS-TENG integrated devices are manufactured to demonstrate the rationality of the selection rules and the reliability of the comprehensive selection series, as shown in Fig. 6a. The movement process of the designed CS-TENG and FS-TENG integrated devices are shown in Supplementary Figs. 19 and 20 (Supplementary Notes 3 and 4), respectively. The best, medium, and worst triboelectric materials in the comprehensive selection series for CS-TENG (PA/FEP, Al/PTFE, and Cu/Kapton) and FS-TENG (PA/FEP, Cu/FEP, Al/PET) are researched. The transferred charge of CS-TENG and FS-TENG prototypes based on the above materials under different relative humidity is shown in Fig. 6b. The results show that: i. the transferred charge from high to low is PA/FEP > Al/PTFE > Cu/Kapton for CS-TENG and PA/FEP > Cu/FEP > Al/PET for FS-TENG; ii. the transferred charge of FS-TENG is more severely impaired by humidity than CS-TENG; iii. the transfer charge of CS-TENG with PA/FEP is improved with increasing relative humidity. These phenomena are the same as the previous experiments. Then, the combined selection coefficients for CS-TENG and FS-TENG integrated devices are calculated (Fig. 6c) and the results give the accuracy and reproducibility of these selection rules. Furthermore, we evaluated the charging capacity of the designed prototypes. As shown in Fig. 6d, CS-TENG integrated device with suitable triboelectric materials (PA/FEP and Al/PTFE) requires 16 s and 46 s to charge the capacitor (4.7  $\mu$ F) to 3 V in 95% RH which is shorter than that in 20% RH. Conversely, the FS-TENG integrated device charging rate in 95% RH is slower than that in 20% RH, but the difference can be reduced by selecting suitable materials. A self-powered system with a CS-TENG (PA/FEP), rectifier bridge, capacitor (100  $\mu$ F), and hygrothermograph is established, and the equivalent circuit diagram is shown in the insert of Fig. 6e. The hygrothermograph can be powered by CS-TENG integrated device with PA/FEP in both 20% RH and 95% RH (Supplementary Movie 4). The charging curve of the capacitor in 20% RH is slower than that in 95% RH, as shown in Fig. 6e. After operation for 36,000 s in 95% RH, the transferred charge of the CS-TENG integrated device with PA/FEP retains 124% of that in 20% RH (Fig. 6f). These results demonstrate that the moisture resistance of TENG can be effectively enhanced by selecting suitable triboelectric materials.



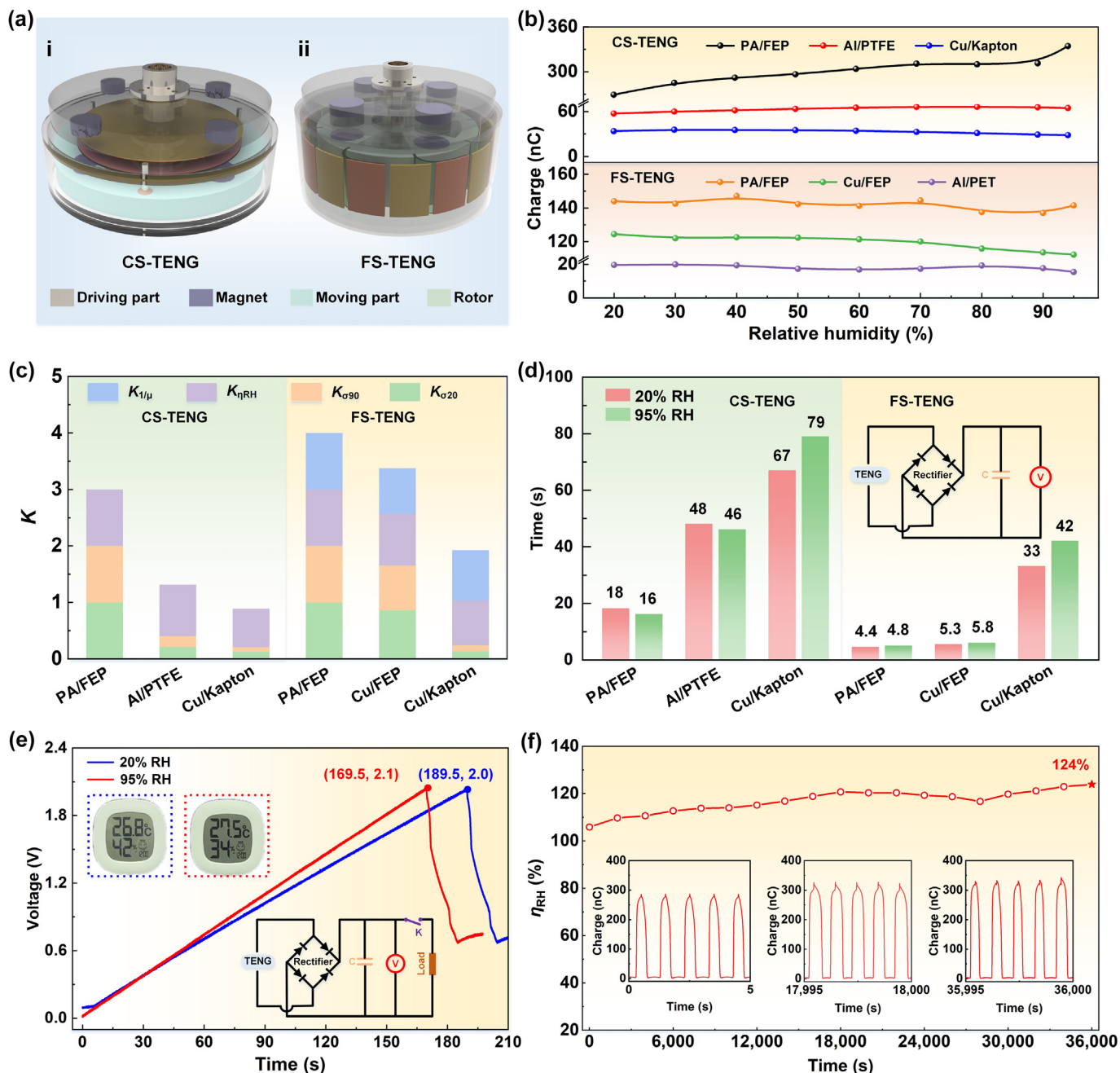


FIGURE 6

**Applications of selected triboelectric materials for TENGs.** **a** Schematic diagram of the designed TENGs integrated devices using the selected triboelectric materials. **b** Influence of the relative humidity on the transferred charge. **c** The combined selection coefficients of designed integrated devices. **d** Charging time of the capacitor by the designed CS-TENG integrated device in 20% RH and 95% RH (4.7  $\mu$ F). **e** Charging curves of a capacitor with 100  $\mu$ F when a hydrothermograph is powered by a CS-TENG integrated device with PA/FEP in 20% RH and 95% RH. **f** Moisture resistance rate of CS-TENG prototype with PA/FEP in 95% RH operation for 36,000 s.

## Conclusions

In summary, we reveal that the continuous water bridge formed between triboelectric materials is the main mechanism affecting the output of TENG at ambient environment. A set of universal material's selection rules have been presented based on charge densities in low and high humid environments, moisture resistance rate, and friction coefficient. The selection rules can screen

whether a triboelectric material pair is appropriate for TENG and determine the comprehensive selection series of triboelectric materials. This selection rule shows that triboelectric materials with high charge density, high moisture resistance rate and low friction coefficient can exhibit high performance at ambient environment. On the basis of the selection rules, TENG with triboelectric materials of PA and FEP shows superior performance.

Moreover, CS-TENG and FS-TENG integrated devices are designed, confirming the practicability of selection rules in practical applications. After working in a high humid environment (95% RH) for 36,000 s, the transferred charge of the CS-TENG integrated device achieves 124% greater than that in a low humid environment (20% RH) and breaks records for previous TENG. The selection rules proposed in this paper will provide a new guideline to select suitable triboelectric materials and promote commercial applications for TENGs at ambient environment. With diversification applications of TENGs, triboelectric materials will become more abundant. The selection rules are not limited to the fifteen types of triboelectric material pairs mentioned in this work, but also apply to any other triboelectric materials. Furthermore, the proposed selection rules will also be applied to select appropriate triboelectric materials for TENG under other alternate environments (e.g., temperature, pressure, pH value, etc.).

## Experimental section

**Fabrication of CS/SE-TENG.** The CS/SE-TENG devices consist of two parts: a static part with triboelectric material II (Cu, PA, and Al), and a moving part with triboelectric material I (PET, Kapton, PDMS, PTFE, FEP). For the static part, an acrylic plate (55 mm × 25 mm) with a thickness of 3 mm is cut by a laser cutting machine (31 Degree 6090). A sponge (50 mm × 20 mm) is pasted on the base, and triboelectric material II with the same size adheres to the sponge. For the moving part, the base is the same as that of the static part, and an electrode (50 mm × 20 mm) is pasted on the base. Triboelectric material I adheres to the electrode, which is designed with an edge 2 mm larger than the electrode to avoid short-circuit when two triboelectric materials are in contact.

**Fabrication of FS/LS-TENG.** The FS/LS-TENG devices consist of two same parts. The moving part of FS/LS-TENG is the same as the static part of CS/SE-TENG. An acrylic plate (85 mm × 60 mm) with a thickness of 3 mm is used as the base of the static part. For FS-TENG, two electrodes (50 mm × 20 mm) are pasted on the base with a separation of 28 mm. Triboelectric material I adheres to the electrodes with a size of 72 mm × 54 mm. For LS-TENG, the electrode and triboelectric material I are the same as that of CS-TENG.

**Fabrication of the CS-TENG integrated device using the selected triboelectric materials.** The material of the lower part of the substrate is acrylic (outer diameter 125 mm, inner diameter 119 mm, height 30 mm). A moving part (diameter 115 mm, thickness 15 mm) with four magnets (diameter 15 mm, thickness 10 mm) is mounted to the base by three steel shafts. A sponge with a diameter of 90 mm is pasted on the moving part and triboelectric material II (Cu, PA, and Al) with a diameter of 90 mm adheres to the sponge. An electrode with a diameter of 90 mm is passed on the top of the base, and triboelectric material I with an edge 2 mm larger adheres to the electrode.

**Fabrication of the FS-TENG integrated device using the selected triboelectric materials.** The material of the lower part of the substrate is acrylic (outer diameter 125 mm, inner diameter 119 mm, height 56 mm). A moving part

(diameter 100 mm, thickness 30 mm) with magnets (diameter 20 mm, thickness 5 mm) is mounted to the base by one steel shaft. Sixteen triboelectric materials II with a width of 35 mm are pasted on an inner wall of the acrylic bucket with a gap of 2 mm. Eight triboelectric materials I with a size of 30 mm × 40 mm are evenly distributed around the moving part.

## Experimental process and measuring equipment.

The humidity and temperature are controlled by a test chamber (Y-HF-960L, Yuhang Zhida). The ultrapure deionized water used in the test chamber is produced by an ultrapure water system (OKP-S020, OKP). The movement processes of CS/SE/FS/LS-TENG and CS/FS-TENG prototypes are achieved by a linear motor (B01-37×166/160, LinMot) and a linear-rotary motor (PR-52, LinMot), respectively. A multi-degree-of-freedom stage (AKV10A-90C, BP-A100, AK25A-10020C, AK25A-10020CZ, Zolix) and a lifting displacement stage (MJ120, Zolix) are used to adjust the contact force of triboelectric materials. A force sensor (ZZ-420, Zhizhan Measurement & Control) is used to measure the contact force between the two triboelectric materials. An electrometer (6514, Keithley) is used to measure the electrical properties of all types of TENGs. A data acquisition system (USB-6218, National Instruments) is used to record the measured results. A friction coefficient meter (MXD-02, Labthink) is used to characterize the friction coefficient. The contact angles are characterized by a contact angle meter (JC2000D, ZYKX). The distribution of water droplets on the surface of PTFE film is observed by microscopy (XSD3, OST).

## Data and materials availability

The data that support the findings of this study are available from the corresponding author upon reasonable request.

## CRedit authorship contribution statement

**Yang Yu:** Conceptualization, Data curation, Investigation, Writing – original draft, Writing – review & editing. **Hengyu Li:** Data curation, Writing – original draft. **Da Zhao:** Data curation, Writing – review & editing. **Qi Gao:** Data curation. **Xiang Li:** Conceptualization. **Jianlong Wang:** Writing – review & editing. **Zhong Lin Wang:** Conceptualization, Resources, Writing – review & editing, Supervision. **Tinghai Cheng:** Conceptualization, Resources, Writing – review & editing, Supervision.

## Data availability

Data will be made available on request.

## Declaration of Competing Interest

The authors declare that they have no known competing financial interests or personal relationships that could have appeared to influence the work reported in this paper.

## Acknowledgements

The authors are grateful for the support received from the National Key R & D Project from Minister of Science and Technology (Nos. 2021YFA1201601 & 2021YFA1201604) and the Beijing Natural Science Foundation (No. 3222023).

## Appendix A. Supplementary material

Supplementary data to this article can be found online at <https://doi.org/10.1016/j.mattod.2023.03.008>.

### References

- [1] C. Zhang et al., *Joule* 5 (2021) 1613–1623.
- [2] X. Liang et al., *Energ. Environ. Sci.* 13 (2020) 277–285.
- [3] F.-R. Fan, Z.-Q. Tian, Z. Lin Wang, *Nano Energy* 1 (2012) 328–334.
- [4] Y. Yu et al., *Mater. Today Phys.* 25 (2022) 100701.
- [5] Z.L. Wang, *Mater. Today* 20 (2017) 74–82.
- [6] D. Liu et al., *Nat. Commun.* 13 (2022) 6019.
- [7] C. Xu et al., *Adv. Mater.* 30 (2018) 1803968.
- [8] S. Lin et al., *Adv. Mater.* 31 (2019) 1808197.
- [9] A.C. Wang et al., *Adv. Funct. Mater.* 30 (2020) 1909384.
- [10] Y. Hu et al., *Nano Energy* 71 (2020) 104640.
- [11] B.-H. Liu et al., *Rare Met.* 40 (2021) 1995–2003.
- [12] V. Nguyen, R. Yang, *Nano Energy* 2 (2013) 604–608.
- [13] L. Liu et al., *Small* 18 (2022) 2201402.
- [14] X. Li et al., *Appl. Energy* 306 (2022) 117977.
- [15] A.R. Mule et al., *Adv. Funct. Mater.* 29 (2019) 1807779.
- [16] P. Chen et al., *Adv. Energy Mater.* 11 (2021) 2003066.
- [17] M.-L. Seol et al., *Small* 10 (2014) 3887–3894.
- [18] D. Kim et al., *Nano Energy* 44 (2018) 228–239.
- [19] Q. Zhou et al., *Nano Energy* 57 (2019) 903–910.
- [20] L. Liu et al., *J. Mater. Chem. A* 9 (2021) 21357–21365.
- [21] J. Wang et al., *Nano Energy* 104 (2022) 107916.
- [22] W. He et al., *Research* 2022 (2022).
- [23] Z. Liu et al., *Nat. Commun.* 13 (2022) 4083.
- [24] G. Khandelwal, N.P. Maria Joseph Raj, S.-J. Kim, *Adv. Energy Mater.* 11 (2021) 2101170.
- [25] H. Zou et al., *Nat. Commun.* 10 (2019) 1427.
- [26] H. Zou et al., *Nat. Commun.* 11 (2020) 2093.
- [27] Z. Zhao et al., *Nat. Commun.* 12 (2021) 4686.
- [28] S. Yong et al., *Adv. Energy Mater.* 11 (2021) 2101194.
- [29] W. Xu et al., *Nature* 578 (2020) 392–396.
- [30] X. Yang et al., *Nano Energy* 60 (2019) 404–412.
- [31] Q. Jiang et al., *Nano Energy* 45 (2018) 266–272.
- [32] J. Shen et al., *Nano Energy* 40 (2017) 282–288.
- [33] Y. Xu et al., *ACS Nano* 15 (2021) 16368–16375.
- [34] Y. Su et al., *Sens. Actuators B Chem.* 251 (2017) 144–152.